Received: 27 May 2020 | Revised: 27 July 2020 | Accepted: 29 July 2020

DOI: 10.1002/qua.26443

FULL PAPER

International Journal of QUANTUM CHEMISTRY WILEY

Oriented external electric fields regulating the oxidation reaction of CH_4 catalyzed by Mn-corrolazine

Xiangqian Wang[1] | Haiyan Wang[1] | Lifeng Zheng[1] | Chun Zhu[1] | Jin-Xia Liang[2]

[1]School of Chemistry and Chemical Engineering, Guizhou University, Guiyang, China

[2]Guizhou Provincial Key Laboratory of Computational Nano-Material Science, Guizhou Education University, Guiyang, China

Correspondence
Chun Zhu, School of Chemistry and Chemical Engineering, Guizhou University, Guiyang 550025, China.
Email: czhu2014@163.com

Jin-Xia Liang, Guizhou Provincial Key Laboratory of Computational Nano-Material Science, Guizhou Education University, Guiyang 550018, China.
Email: liangjx2009@163.com

Funding information
Natural Science Foundation of Guizhou Province, Grant/Award Number: [2017]1029; National Natural Science Foundation of China, Grant/Award Numbers: 21963005, 21763006, 21663008

Abstract

Mn-corrolazine-catalyzed CH_4 oxidation, as well as the regulation of its oriented external electric fields (OEEFs), is systematically studied using the first-principle calculations. Extensive density functional calculations show that the activation energy of CH_4 oxidation catalyzed by Mn-corrolazine is up to 38.5 kcal/mol in the field-free condition. However, when the OEEF is applied, the reactant and the transition state of the oxidation reaction are stabilized, originating from an attractive interaction between the increased dipole moment and the applied fields. Furthermore, when the field is negative, the activation energy decreases as the field increases. Especially for the negative field along the intrinsic Mn—O reaction axis perpendicular to the corrolazine ring, of which the orientation is easily aligned in practical applications, when its intensity reaches −0.015 a.u., the activation energy of CH_4 oxidation is reduced to 25.0 kcal/mol.

KEYWORDS
catalysis, CH_4 oxidation, density functional theory calculations, Mn-corrolazine, oriented external electric field

1 | INTRODUCTION

Searching for novel and efficient catalysts has always been the most important subject in chemical research. Traditionally, the common catalysts are molecules and the surfaces or interface in homogeneous and heterogeneous systems,[1–6] respectively. However, in recent years, many new technologies, such as ultrasound,[7] microwaves,[8] mechanical stress,[9] and nanoreactors,[10] have been used to control various reaction processes as novel catalysts. Electrostatic forces play an extremely important role in chemical reactions involving the arrangement of nuclei and electrons.[11–13] A typical example is the electrostatic catalysis of enzymes in nature.[10,14–16] The polar environment originating from the subtle arrangement of atoms around the active site produces the electric field that can efficiently and selectively catalyze various biochemical reactions. Using the same idea, research is increasingly focused on regulating the stability of the reactants and transition states, as well as products, using artificial external electric fields through dipole-field interaction, thereby manipulating the chemical reaction process.[17–44]

Very recently, Shaik et al. performed a much computational research to explore the effect of oriented external electric fields (OEEFs) on organic reactions.[17–23] Their research results show that OFFEs along the reaction axis involving the electron transfer can significantly catalyze the organic reactions, while the OFFEs along other directions can control the regioselectivity and stereoselectivity, and some results are confirmed by experimental evidence provided by Aragonès et al.[18] However, although great progress has been made in both the experimental and theoretical research,[17–24,27,30] a major problem in using the OFFEs to manipulate reaction processes is to deliver the external electric fields and orient the molecules within the applied fields simultaneously.

The corrole, a porphyrinoid macrocyclic aromatic compound consisting of four conjugated pyrrole rings, has received increasing attention due to its superior photoelectric properties and catalytic properties. The corrole has a smaller cavity compared with the porphyrin because of the lack of one meso-carbon atom. The structural feature makes it well able to stabilize high-valence metals, resulting in its high catalytic performance,

and several studies have been carried out to improve its catalytic efficiency through the structural modification of meso and β-position substitution. Recently, a new corrole derivative, corrolazine, was synthesized experimentally by substituting the meso-C atoms of corrole with N atoms, which further stimulated the research of corrole in the field of catalysis. Prokop and Goldberg's experiment and our density functional theory (DFT) calculations show that the high-valence Mn(V)-oxo corrolazine complex can be conveniently formed by the oxidation of the Mn(III) corrolazine with O_2 under visible light irradiation, while organic substrates are oxidized through continuous H-abstraction and rebound processes.[45,46] Therefore, Mn corrolazine is of great significance in catalysis because it can directly use cost-effective, abundant, and environmentally friendly molecular O_2 as an oxidant. Moreover, in the process of Mn-corrolazine-catalyzed oxidation of organic substrates, the rate-determining step is through the Mn-corrolazine—O—O species bearing the instinct Mn—O reaction axis. Thus, if the Mn corrolazine is fixed on the surface of two-dimensional materials, its catalytic reaction may be easily regulated by the external electric field along the instinct axis.

Here, in order to investigate the mechanism of the external electric field regulating Mn-corrolazine-catalyzed reactions, DFT calculations have been carried out to study the selective oxidation reaction: CH_4 + [Mn(III)]-O-O → Mn(V)-oxo + CH_3OH in external electric fields along different directions, which provides the theoretical foundation for further expanding the application of Mn-corrolazine catalysis regulated by the external electric field along the intrinsic Mn—O reaction axis.

2 | COMPUTATIONAL DETAILS

All calculations of the reaction were carried out with the Gaussian 16 program using the B3LYP hybrid functional and the effective core potential coupled with the LANL2DZ basis set for manganese and the all-electron 6-31G++(d,p) basis set for other atoms.[47–49] The geometries of the reactant complex (RC), transition state (TS), and product (P) were fully optimized without any symmetry constraints. Frequency calculations were performed at the same level of theory to ascertain the nature of the stationary points on the potential energy surface, where there are only real frequencies for all RC and P species, and only one imaginary frequency for all TS species. Moreover, all TS species were further verified by intrinsic reaction coordinate (IRC) calculations.

The effects of OEEFs applied along two Cartesian axes with both positive and negative directions on the oxidation reaction of CH_4 were studied using the keyword "Field = M ± N". The orientations of the two applied axes were shown in Scheme 1. The F_{z1} axis is along the O—O bond of the transition state, and the F_{z2} axis is along the intrinsic Mn—O reaction axis perpendicular to the corrolazine ring. The positive direction of the electric field vector follows the convention of Gaussian 16, which is also shown in Scheme 1. The electric field intensity ranges from −0.0150 a.u to +0.0150 a.u. for F_{z1} and F_{z2} (1 a.u. = 51.4 V/Å).

3 | RESULTS AND DISCUSSION

3.1 | The reaction of [Mn]—O—O corrolazine with CH_4 under the field-free condition

According to our previous studies,[46,50–52] the organic substrate oxidation reaction catalyzed by Mn-corrolazine was through the [Mn]—O—O species. Then, we studied the reaction between [Mn]—O—O and CH_4 in the absence of OEEF. As shown in the Figure 1 and Table 1, the terminal

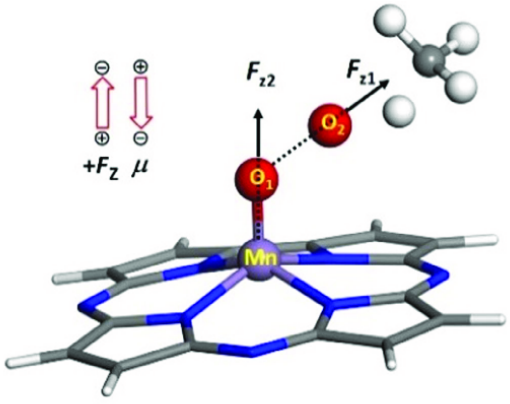

SCHEME 1 Definitions of two OEEFs. F_{z1} is along the O—O bond in the TS, and F_{z2} is along the Mn—O bond perpendicular to the corrolazine ring. The inset indicates the definition of a positive OEEF $F_z > 0$ and the stabilizing orientation of the dipole moment μ_z. OEEFs, oriented external electric fields; TS, transition state

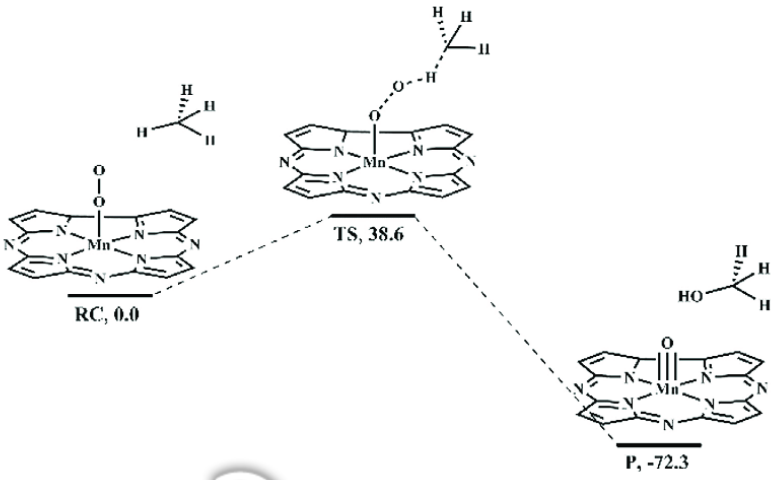

FIGURE 1 The predicted reaction pathway of [Mn]—O—O corrolazine with CH_4 under the electric field-free condition

TABLE 1 Selected Bond lengths (Å) and the relative electronic energies (ΔE, kcal/mol) of species involved in the reaction of [Mn]—O—O and CH_4

State	d_{Mn-O1}	d_{O1-O2}	d_{O2-H}	d_{H-C}	ΔE
RC	1.607	1.261	2.640	1.094	0.0
TS	1.557	1.728	1.283	1.203	38.6
P	1.534	2.945	0.970	1.957	−72.3

Abbreviations: P, product; RC, reactant complex; TS, transition state.

O of Mn—O—O first abstracts a hydrogen of CH_4, and the O—O bond length increases significantly, while the distance between the O and H atoms decreases from 2.640 Å in the RC to 1.283 Å in the TS, and the activation energy is up to 38.5 kcal/mol. Then, the CH_3OH is produced along with the formation of Mn(V) – oxo corrolazine by rebound reaction where the newly generated OH is rapidly rebounded to the substrate because the CH_3• does not have enough time to leave the [Mn]—O—O—H moiety originating from the high reaction rate of rebound reaction.[52–54] Moreover, the reaction energy of 72.3 kcal/mol will promote the reaction to the right thermodynamically. The reaction pathway was further verified by IRC calculation. Furthermore, the desorption energy of the methanol product is calculated by Formula (1), which is only 5.8 kcal/mol, indicating that the desorption of methanol product is easy.

$$E_{de} = E_P - E_{CH_3OH} - E_{Mn-oxo\ corrolazine} \quad (1)$$

where E_P and E_{CH_3OH} are the energies of the product and the isolated CH_3OH, respectively, and $E_{Mn-oxo\ corrolazine}$ denotes the energy of the isolated Mn-oxo corrolazine.

3.2 | The effect of OEEF on the stabilities of the reactant and transition state of the reaction of [Mn]—O—O with CH_4

We considered the effects of OEEFs along two axes, F_{z1} and F_{z2}, in positive and negative directions on the stability of the TS of the reaction of [Mn]—O—O with CH_4. As Figure 2 shows, the application of OEEFs has a significant effect on the relative electronic energy of the TS. For F_{z1} and $F_{z2} > 0$, the OEEF stabilizes TS, and the relative electronic energy of TS decreases as the electric field intensity increases. While for F_{z1} and $F_{z2} < 0$, the situation becomes complex, in which the OEEFs in different axes exhibit different behaviors, for F_{z1}, the OEEF stabilizes the TS and decreases its relative electronic energy as the field intensity increases. For F_{z2}, in the initial part of $F_{z2} < 0$ range, the OEEF destabilizes the TS and raises its relative electronic energy. However, as the intensity of the OEEF is further increased to more than −0.002 a.u., the OEEF stabilizes the TS and decreases its relative electronic energy again as shown in the inset in Figure 2. For exploring the internal reason of the stability change of the TS influenced by the OEEFs, we analyze the change of dipole moment in z orientation of the TS with the change of the OEEF. As shown in Figure 2, for F_{z1} and $F_{z2} > 0$, the dipole moment in z1 orientation of the TS is increased from −1.11 D without an electric field to −21.25 D in $F_{z1} = 0.015$

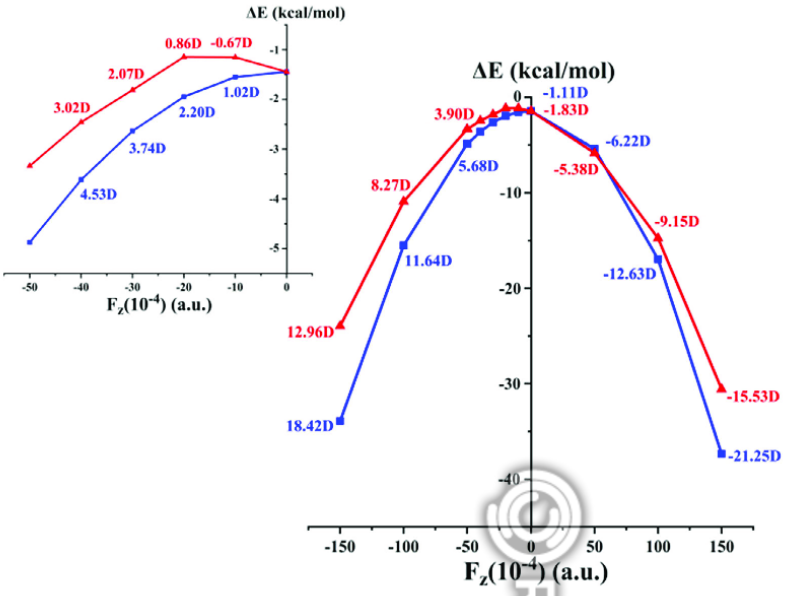

FIGURE 2 Plots of the relative energies of TS as a function of the applied OEEFs with the dipole moments (debye, D) at the selected OEEF values; blue for F_{z1} and red for F_{z2}. The inset is the enlarged view at F_{z1} and F_{z2} = –0.005 a.u. to 0 a.u. OEEFs, oriented external electric fields; TS, transition state

TABLE 2 The partial atomic Mulliken charge populations (|e⁻|) and the dipole moments μ_z (debye, D) of the transition state (TS) in the electric field-free condition and F_{z1} and F_{z2} = ± 0.015 a.u.

F_z (10^{-4}) (a.u.)	0.015	0	–0.015
Mn (z1/z2)	0.09/0.04	0.01	–0.11/–0.42
O1 (z1/z2)	0.10/0.05	0.15	0.27/0.44
O2 (z1/z2)	–0.40/–0.52	–0.29	–0.2/–0.13
H (z1/z2)	0.50/0.47	0.41	0.29/0.32
C (z1/z2)	–1.08/–1.01	–0.88	–0.72/–0.76
$\Delta\mu_z$(z1/z2)	18.42/12.96	–1.11/–1.83	–21.25/–15.53

(from –1.83 D to –15.53 D in F_{z2} = 0.015 in z2 orientation). Thus, the F_{z1} and F_{z2} > 0 stabilizing the TS originates from the attraction between the increased dipole moment in z orientation and the external electric field. When flipping the electric field to F_{z2} < 0 decreases the dipole moment in z2 orientation of the TS at the initial part of the OEEF, the repulsion between F_{z2} and dipole moment destabilizes the TS. However, as F_{z2} is made increasingly more negative, the molecular dipole in z2 orientation flips its direction at the critical F_{z2} value of 0.002 a.u., such that the F_{z2} < 0 increases the dipole moment in z2 orientation, and the TS is stabilized again. For F_{z1} < 0, the OEEF reverses the molecular dipole in z1 orientation even at the weaker electric field of 0.001 a.u., thereby stabilizing the TS.

To further understand the electronic origin of these changes, Mulliken charge population analysis for the TS in the electric field-free condition and F_{z1} and F_{z2} = ±0.015 a.u. was carried out. As Table 2 shows, in the electric field-free condition, the Mn atom has a slight positive charge of 0.01 |e⁻|, the C atom of CH_4 has a negative charge of 0.88 |e⁻|, and the molecular dipole in z1 orientation of the TS is –1.11 D (–1.83 D in z2 orientation). With F_{z1} and F_{z2} = +0.015, the Mn atom becomes slightly more positive, with a positive charge of 0.09 |e⁻| for F_{z1} (0.04 |e⁻| for F_{z2}), while the C atom of CH_4 becomes significantly more negative, with a negative charge of -1.08 |e⁻| for F_{z1} (–1.01 |e⁻| for F_{z2}). Therefore, the dipole moment in z orientation of the TS is increased to –21.25 D for F_{z1} (–15.53 D for F_{z2}). Flipping the electric field to F_{z1} and F_{z2} = –0.015 a.u. depletes the negative charge of the C atom of CH_4 and flips the positive to negative charge of the Mn atom (–0.11 |e⁻| for F_{z1}, –0.42 |e⁻| for F_{z2}). Thus, the charge transfer flips the dipole moment in z orientation of TS, which varies from –1.11 D to 18.42 D for F_{z1} and from –1.83 D to 12.96 D for F_{z2}. In addition, as the electron transfer occurs from [Mn]—O—O corrolazine moiety to CH_4 moiety, the Mulliken charge of the C atom of CH_4 is –0.88|e⁻|, resulting in an internal electric field. Then, when the external electric fields are applied, the Mulliken charges of the C atom of CH_4 are –0.88, –1.08, and –0.72 |e⁻| under fields of +0.015, 0.0, and –0.015 a.u. for F_{z1} (–1.01, –0.88, –0.76 |e⁻| for F_{z2}), respectively, which is

consistent with the work of Jiang et al.[55] that the positive external electric field enhances the electron transfer in the positive Z-direction, and the negative external electric field weakens the electron transfer in the positive Z-direction.

Similar to the effect on the TS, the OEEFs also have remarkable influence on the stability of RC of the reaction of [Mn]—O—O with CH_4. As shown in Figure 3, for F_{z1} and $F_{z2} > 0$, as the OEEFs in both axes F_{z1} and F_{z2} increase, the dipole moment in z orientation of the RC increases rapidly. Then, the stability of the RC increases, resulting from the attractive interaction between the OEEFs and the increased dipole moment in z orientation. For F_{z1} and $F_{z2} < 0$, the dipole moment in z orientation first decreases with the increase of the electric field intensity. When the electric field exceeds the critical value (0.001 a.u. for F_{z1} and 0.004 a.u. for F_{z2}), the dipole moment in z orientation reverses, and its intensity increases with the increase of the intensity of the applied OEEF. Therefore, the stability of RC first weakens and then strengthens with the increase of the field intensity.

3.3 | The effect of OEEF on the activation energy of the reaction of [Mn]—O—O with CH4

We further investigate the effect of the OEEFs on the activation energy of the reaction of [Mn]—O—O with CH_4. As Figure 4 shows, for $F_{z1} > 0$, the reaction activation energy increases slightly with the increase of the field intensity in the initial part of F_{z1}. This is because the dipole moments in z1 orientation of the RC and TS increases with the increase of the field intensity, and the dipole moment in z1 orientation of the RC is larger than that of the TS, except that, at F_{z1} = 0.005 a.u., the dipole moments in z1 orientation of the RC and TS are approximately equal, as shown in Table 3. However, as the applied F_{z1} becomes stronger than 0.010 a.u., the dipole moment in the z1 orientation of the TS is already larger than that of RC. Thus, the reaction activation energy decreases slightly with the increase of F_{z1} as shown in Figure 4. For $F_{z2} > 0$, the dipole moments in z2 orientation of the RC and TS increase with the increase of the field intensity, and the dipole moment in z2 orientation of the RC is always larger than that of the TS. Therefore, the activation always increases slightly with an increase of the electric field intensity. For F_{z1} and $F_{z2} < 0$, both F_{z1} and F_{z2} decrease the activation energy, which is a result of the dipole moments in z orientation of the RC and TS increasing with the increase in the field intensity, and the dipole moment in z orientation of the TS is always larger than that of the RC, as shown in Table 3. Thus, the range of OEEF <0 promotes the CH_4 oxidation reaction. Especially for F_{z2}, its effect on the reaction is more pronounced than that of F_{z1} as demonstrated by the slopes of the curves in Figure 4, in which the curve slop for F_{z2} is larger than that for F_{z1}, and its orientation is approximately perpendicular to the corrolazine ring, which is more easily aligned in practical applications. These features make it easier to regulate the oxidation reaction of CH_4, and the activation energy of the reaction is even reduced to 25.0 kcal/mol when the F_{z2} reaches –0.015 a.u.

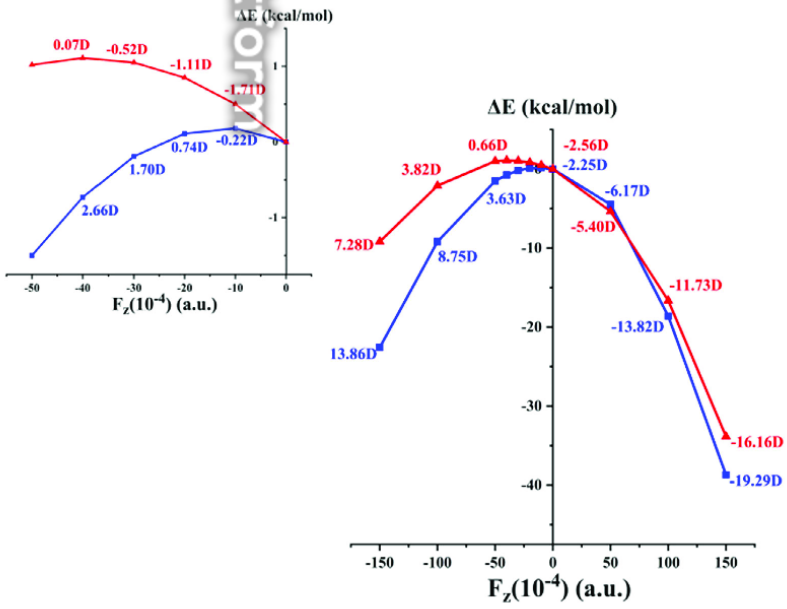

FIGURE 3 Plots of the relative energies of RC as a function of the applied OEEFs with the dipole moments (debye, D) at the selected OEEF values; blue for F_{z1} and red for F_{z2}. The inset is the enlarged view at F_{z1} and F_{z2} = –0.005 a.u. to 0 a.u. OEEFs, oriented external electric fields; RC, reactant complex

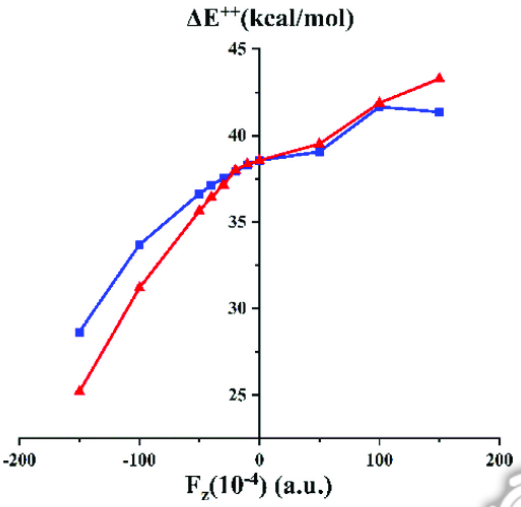

FIGURE 4 Plots of the activation energy of the reaction of [Mn]—O—O with CH_4 as a function of the applied OEEFs; blue curve for F_{z1} and red curve for F_{z2}. OEEFs, oriented external electric fields

	F_{z1}		F_{z2}	
F_z (10^{-4}) (a.u.)	$\Delta\mu_{z1}$ (RC)	$\Delta\mu_{z1}$ (TS)	$\Delta\mu_{z2}$ (RC)	$\Delta\mu_{z1}$ (TS)
150	−19.29	−21.25	−16.16	−15.53
100	−13.82	−12.63	−11.73	−9.15
50	−6.17	−6.22	−5.40	−5.38
0	−2.25	−1.11	−2.56	−1.83
−10	−0.22	1.02	−1.71	−0.67
−20	0.74	2.20	−1.11	0.86
−30	1.70	3.74	−0.52	2.07
−40	2.66	4.53	0.07	3.02
−50	3.63	5.68	0.66	3.90
−100	8.75	11.64	3.82	8.27
−150	13.86	18.42	7.28	12.96

TABLE 3 The dipole moments μ_z (Debye, D) in z orientation of RC and TS in the electric field-free condition in F_{z1} and in F_{z2}

Abbreviations: RC, reactant complex; TS, transition state.

4 | CONCLUSIONS

The catalytic oxidation of CH_4 is an extremely important research topic in catalysis. Here, we first studied the reaction of [Mn]—O—O with CH_4 in field-free condition and found that its activation energy is high, reaching 38.5 kcal/mol. Then, we used the OEEFs along the Mn—O axis and O—O axis to regulate the oxidation reaction. When the positive field is applied, the dipole moments of the reactant and the TS increase as the intensity of the field increases, and the reactant and the transition state are stabilized, resulting from the attractive interaction between the field and the dipole moments. When the negative field is applied, the dipole moments of the reactant and TS decrease with the increase of the field in a weak field. However, as the field becomes stronger, the dipole moments reverse, and the intensities in turn increase as the intensity of the field increases. Therefore, the reactant and the TS are destabilized in initial weak field and then stabilized again as the intensity of the field increases. Furthermore, the variation of the reaction activation energy with the field is investigated. When the field is positive, the activation energy is slightly increased. When the field is negative, the activation decreases with the increase of the intensity of the field. Especially for the OEEF along the intrinsic Mn—O reaction axis, its orientation is approximately perpendicular to the corrolazine ring, which is more easily aligned in practical applications, and when the field reaches −0.015 a.u., the activation energy of the reaction is even reduced to 25.0 kcal/mol. These features make it easier to regulate the oxidation reaction of CH_4.

ACKNOWLEDGMENTS

This work was supported by the National Natural Science Foundation of China (Nos. 21663008, 21763006, and 21963005) and Natural Science Foundation of Guizhou Province of China (No. [2017]1029). We are grateful for the computational resources provided by the State Key Laboratory of Physical Chemistry of Solid Surfaces (Xiamen University) and the Shanghai Super-computing Center.

AUTHOR CONTRIBUTIONS

Xiangqian Wang: Data curation; investigation; writing-original draft. **Haiyan Wang:** Data curation; investigation. **Lifeng Zheng:** Data curation. **Chun Zhu:** Conceptualization; funding acquisition; project administration. **Jin-Xia Liang:** Conceptualization; funding acquisition.

ORCID

Chun Zhu https://orcid.org/0000-0002-2914-2438

REFERENCES

[1] M. Xing, L. Guo, Z. Hao, *Int. J. Quantum Chem.* **2018**, *118*, e25767.
[2] H. Zhang, H. Bai, Y. Guo, D. Wei, H. Chen, Y. Zhu, W. Zhang, *Int. J. Quantum Chem.* **2019**, *119*, e25836.
[3] H. Li, J. Qin, Y. Zhang, S. Xu, J. Du, J. Tang, *RSC Adv.* **2018**, *8*, 39352.
[4] M. Fadel, J.-V. Daurelle, V. Fourmond, J. Z. M. Vicente, *Phys. Chem. Chem. Phys.* **2019**, *21*, 12360.
[5] M. V. Reddy, S. M. Kang, S. Yoo, S. S. Woo, D. W. Kim, *RSC Adv.* **2019**, *9*, 9435.
[6] N. He, Y. Zhu, Z. Zhu, Y. Yang, W. Zhang, D. Wei, L. Qu, M. Tang, H. Chen, *Int. J. Quantum Chem.* **2019**, *119*, e26039.
[7] T. J. Mason, *Chem. Soc. Rev.* **1997**, *26*, 443.
[8] M. Larhed, C. Moberg, A. Hallberg, *Acc. Chem. Res.* **2002**, *35*, 717.
[9] J. Wang, T. B. Kouznetsova, Z. Niu, M. T. Ong, H. M. Klukovich, A. L. Rheingold, T. J. Martinez, S. L. Craig, *Nat. Chem.* **2015**, *7*, 323.
[10] S. H. Petrosko, R. Johnson, H. White, C. A. Mirkin, *J. Am. Chem. Soc.* **2016**, *138*, 7443.
[11] C. Hadad, E. Florez, N. Acelas, G. Merino, A. Restrepo, *Int. J. Quantum Chem.* **2019**, *119*, e25766.
[12] J. Camacho Gonzalez, S. Mondal, F. Ocayo, R. Guajardo-Maturana, A. Muñoz-Castro, *Int. J. Quantum Chem.* **2020**, *120*, e26080.
[13] Y. Park, H. Kang, H. Kang, *J. Phys. Chem. C* **2020**, *124*, 1129.
[14] I. T. Suydam, C. D. Snow, V. S. Pande, S. G. Boxer, *Science* **2006**, *313*, 200.
[15] S. D. Fried, S. G. Boxer, *Annu. Rev. Biochem.* **2017**, *86*, 387.
[16] V. Vaissier Welborn, T. Head-Gordon, *Chem. Rev.* **2019**, *119*, 6613.
[17] S. Shaik, S. P. De Visser, D. Kumar, *J. Am. Chem. Soc.* **2004**, *126*, 11746.
[18] W. Lai, H. Chen, K. B. Cho, S. Shaik, *J. Phys. Chem. Lett.* **2010**, *1*, 2082.
[19] R. Meir, H. Chen, W. Lai, S. Shaik, *ChemPhysChem* **2010**, *11*, 301.
[20] S. Shaik, D. Mandal, R. Ramanan, *Nat. Chem.* **2016**, *8*, 1091.
[21] R. Ramanan, D. Danovich, D. Mandal, S. Shaik, *J. Am. Chem. Soc.* **2018**, *140*, 4354.
[22] Z. Wang, D. Danovich, R. Ramanan, S. Shaik, *J. Am. Chem. Soc.* **2018**, *140*, 13350.
[23] T. Stuyver, D. Danovich, F. De Proft, S. Shaik, *J. Am. Chem. Soc.* **2019**, *141*, 9719.
[24] A. C. Aragonès, N. L. Haworth, N. Darwish, S. Ciampi, N. J. Bloomfield, G. G. Wallace, I. Diez-Perez, M. L. Coote, *Nature* **2016**, *531*, 88.
[25] S. Lakshmi, S. Dutta, S. K. Pati, *J. Phys. Chem. C* **2008**, *112*, 14718.
[26] C. F. Gorin, E. S. Beh, M. W. Kanan, *J. Am. Chem. Soc.* **2012**, *134*, 186.
[27] R. Garcia, N. S. Losilla, J. Martínez, R. V. Martinez, F. J. Palomares, Y. Huttel, M. Calvaresi, F. Zerbetto, *Appl. Phys. Lett.* **2010**, *96*, 143110.
[28] M. Akamatsu, N. Sakai, S. Matile, *J. Am. Chem. Soc.* **2017**, *139*, 6558.
[29] S. Ciampi, N. Darwish, H. M. Aitken, I. Díez-Perez, M. L. Coote, *Chem. Soc. Rev.* **2018**, *47*, 5146.
[30] L. Zhang, E. Laborda, N. Darwish, B. B. Noble, J. H. Tyrell, S. Pluczyk, A. P. Le Brun, G. G. Wallace, J. Gonzalez, M. L. Coote, *J. Am. Chem. Soc.* **2018**, *140*, 766.
[31] D. Rai, H. Joshi, A. D. Kulkarni, S. P. Gejji, R. K. Pathak, *J. Phys. Chem. A* **2007**, *111*, 9111.
[32] K. Bhattacharyya, S. Karmakar, A. Datta, *Phys. Chem. Chem. Phys.* **2017**, *19*, 22482.
[33] L. J. Yu, M. L. Coote, *J. Phys. Chem. A* **2019**, *123*, 582.
[34] M. X. Zhang, H. L. Xu, *J. Comput. Chem.* **2019**, *40*, 1772.
[35] T. Xu, R. Momen, A. Azizi, T. van Mourik, H. Früchtl, S. R. Kirk, S. Jenkins, *J. Comput. Chem.* **2019**, *40*, 1881.
[36] C. Foroutan-Nejad, V. Andrushchenko, M. Straka, *Phys. Chem. Chem. Phys.* **2016**, *18*, 32673.
[37] B. Schirmer, S. Grimme, *Chem. Commun.* **2010**, *46*, 7942.
[38] A. A. Arabi, C. F. Matta, *Phys. Chem. Chem. Phys.* **2011**, *13*, 13738.
[39] H. Li, T. A. Su, V. Zhang, M. L. Steigerwald, C. Nuckolls, L. Venkataraman, *J. Am. Chem. Soc.* **2015**, *137*, 5028.
[40] C. Wang, D. Danovich, H. Chen, S. Shaik, *J. Am. Chem. Soc.* **2019**, *141*, 7122.
[41] S. Shaik, R. Ramanan, D. Danovich, D. Mandal, *Chem. Soc. Rev.* **2018**, *47*, 5125.
[42] F. Che, J. T. Gray, S. Ha, N. Kruse, S. L. Scott, J. S. McEwen, *ACS Catal.* **2018**, *8*, 5153.
[43] F. Che, J. T. Gray, S. Ha, J. S. McEwen, *ACS Catal.* **2017**, *7*, 551.
[44] M.-X. Zhang, H.-L. Xu, Z.-M. Su, *Int. J. Quantum Chem.* **2020**, *120*, e26134.
[45] K. A. Prokop, D. P. Goldberg, *J. Am. Chem. Soc.* **2012**, *134*, 8014.
[46] C. Zhu, J.-X. Liang, Z. Cao, *J. Phys. Chem. C* **2018**, *122*, 20781.
[47] M. J. Frisch, G. W. Trucks, H. B. Schlegel, G. E. Scuseria, M. A. Robb, J. R. Cheeseman, G. Scalmani, V. Barone, G. A. Petersson, H. Nakatsuji, X. Li, M. Caricato, A. V. Marenich, J. Bloino, B. G. Janesko, R. Gomperts, B. Mennucci, H. P. Hratchian, J. V. Ortiz, A. F. Izmaylov, J. L. Sonnenberg, F. D.

Williams, F. Lipparini, F. Egidi, J. Goings, B. Peng, A. Petrone, T. Henderson, D. Ranasinghe, V. G. Zakrzewski, J. Gao, N. Rega, G. Zheng, W. Liang, M. Hada, M. Ehara, K. Toyota, R. Fukuda, J. Hasegawa, M. Ishida, T. Nakajima, Y. Honda, O. Kitao, H. Nakai, T. Vreven, K. Throssell, J. A. Montgomery Jr., J. E. Peralta, F. Ogliaro, M. J. Bearpark, J. J. Heyd, E. N. Brothers, K. N. Kudin, V. N. Staroverov, T. A. Keith, R. Kobayashi, J. Normand, K. Raghavachari, A. P. Rendell, J. C. Burant, S. S. Iyengar, J. Tomasi, M. Cossi, J. M. Millam, M. Klene, C. Adamo, R. Cammi, J. W. Ochterski, R. L. Martin, K. Morokuma, O. Farkas, J. B. Foresman, D. J. Fox, *Gaussian 16 Literature Citation*, Gaussian, Inc., Wallingford, CT **2016**.

[48] C. Lee, W. Yang, R. G. Parr, *Phys. Rev. B: Condens. Matter* **1988**, *37*, 785.

[49] J. Paier, M. Marsman, G. Kresse, *J. Chem. Phys.* **2007**, *127*, 024103.

[50] J.-X. Liang, Y. Wu, H. Deng, C. Long, C. Zhu, *RSC Adv.* **2019**, *9*, 1373.

[51] C. Zhu, J.-X. Liang, G. Wei, *Phys. Chem. Chem. Phys.* **2016**, *18*, 12338.

[52] C. Zhu, J. Liang, B. Wang, J. Zhu, Z. Cao, *Phys. Chem. Chem. Phys.* **2012**, *14*, 12800.

[53] S. Shaik, D. Kumar, S. P. de Visser, A. Altun, W. Thiel, *Chem. Rev.* **2005**, *105*, 2279.

[54] J. P. T. Zaragoza, T. H. Yosca, M. A. Siegler, P. Moënne-Loccoz, M. T. Green, D. P. Goldberg, *J. Am. Chem. Soc.* **2017**, *139*, 13640.

[55] C. -H. Yeh, T. M. L. Pham, S. Nachimuthu, J.-C. Jiang, *ACS Catal.* **2019**, *9*, 8230.

How to cite this article: Wang X, Wang H, Zheng L, Zhu C, Liang J-X. Oriented external electric fields regulating the oxidation reaction of CH_4 catalyzed by Mn-corrolazine. *Int J Quantum Chem*. 2021;121:e26443. https://doi.org/10.1002/qua.26443